4.1 INTRODUCTION

This chapter explores the effect of build orientation on the tensile and low cycle fatigue (LCF) behavior of additive manufactured maraging steel and compares with the behavior of conventionally manufactured (CM) maraging steel. The effect of heat treatment on tensile and fatigue properties is also investigated. Overall, this chapter provides valuable insights into the effect of build orientation and heat treatment on the mechanical behavior of additive manufactured maraging steel samples, which can aid in the design and optimization of additive manufacturing processes for high-performance applications experiencing monotonic and cyclic loading.

Tensile testing of AM maraging steel was performed in as-built (AB) and heat treated (HT) conditions in three orientations, at room temperature at a strain rate of 10^{-3} s^{-1}. LCF testing of AB and HT samples in all three orientations was carried out at fixed strain amplitude (±0.5%) and strain rate (5×10^{-3} s^{-1}). Fracture surfaces of the both LCF and tensile tested specimens were analyzed using scanning electron microscope operating at 20kV.

4.2 Influence of Build Orientation on Tensile Behaviour

4.2.1 Residual stresses

In the current study, it is found that a significant amount of compressive residual stresses was generated in as-built AM samples. The residual stresses increased as a function of build orientation in as-built AM samples as shown in Table 4.1. However, after heat treatment, the residual stresses in the as built AM samples were found to be almost relieved.

Table 4.1 Values of residual stress in AB and HT samples.

Sample	Residual Stress (MPa)
0° AB	-304.1 ± 10.1
45° AB	-485.0 ± 14.6
90° AB	-585.2 ± 22.3
0° HT	-0.3 ± 8.3
45° HT	-0.1 ± 10.4
90° HT	0.5 ± 12.2

4.2.2 Hardness

The microhardness values of CM and AM samples in three conditions, i.e. as-built/as received, solution-treated (ST) and solution-treated plus aged (HT) conditions are shown in the form of a bar diagram in Fig.4.1. Hardness was found to be the highest i.e., 377±6.5 HV in as-built sample in 90° AB orientation. Lower values of hardness were found in other samples. The values are 331±10 HV in the as-built 45° AB sample, 314±7 HV in as-built 0° AB and 302±4.2 HV in CM samples. After heat treatment, CM-HT sample showed the highest hardness (587±11.1 HV) and AM-HT samples showed an average hardness of 552 HV in all orientations.

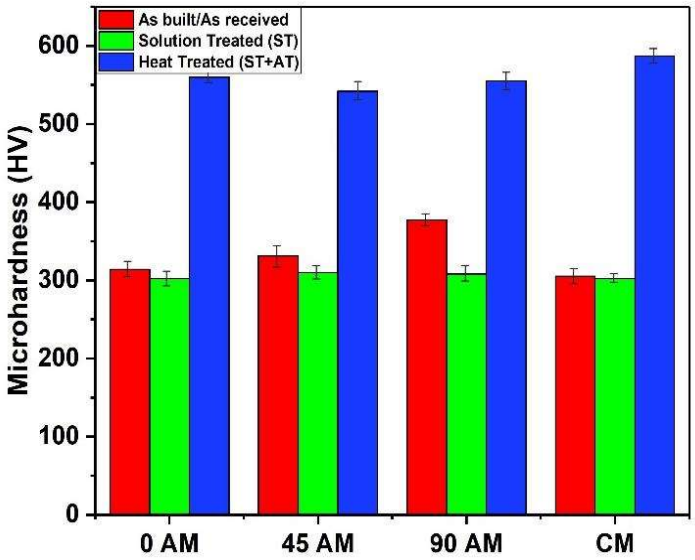

Fig. 4.1 Variation of microhardness in different conditions of CM and AM samples.

4.2.3 Tensile behaviour

Engineering tensile stress-strain curves of AB and HT conditions of AM and CM samples are shown in Figs. 4.2, 4.3 and 4.4. Tensile properties of AB samples in different build orientations and CM samples are shown in Table. 4.2. Sample built in 0° orientation, i.e. 0° AB sample showed maximum elongation before fracture followed by 45° AB and 90° AB samples. The 45° AB samples showed better strength followed by 0° AB and 90° AB samples. Maximum degree of work hardening was observed for 0° AB samples, as shown in Table 4.2.

The Engineering stress-strain curves of heat-treated additive samples in 0°, 45° and 90° build orientations are presented in Fig. 4.3. There was very little difference observed in yield and tensile strength of HT samples. The difference in ductility parameters is significant in 0°, 45° and 90° HT samples, as shown in Fig. 4.3. Maximum degree of work hardening was observed for 45° HT samples among HT additive manufactured samples. Also, the 45° HT samples showed maximum uniform elongation before necking.

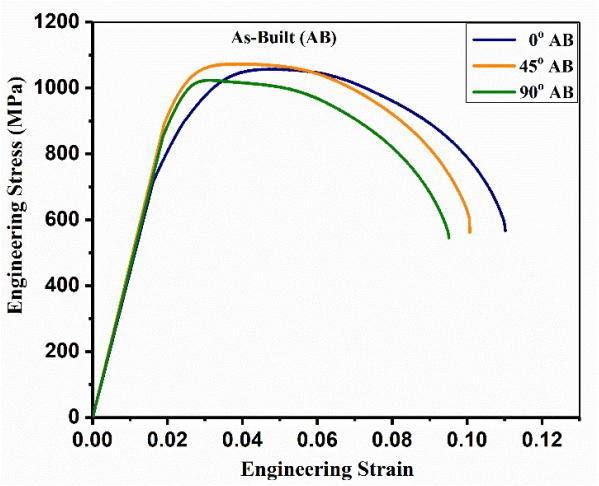

Fig. 4.2 Engineering stress-strain curves of AB samples of M300 steel in different orientations.

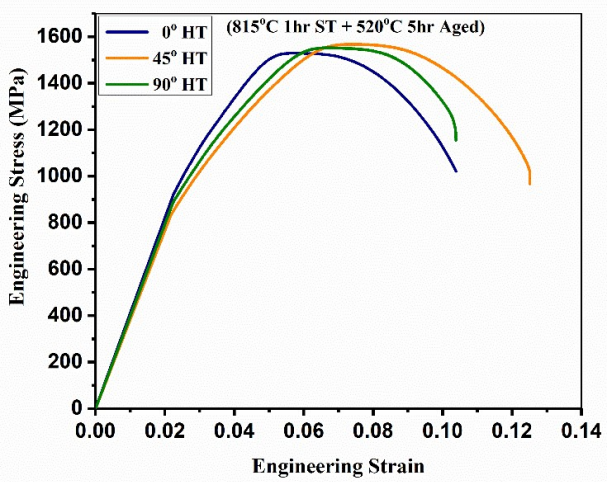

Fig. 4.3. Engineering stress-strain curves of AM-HT samples of M300 steel in different orientations.

It can be observed from Table. 4.2, that all as-built (AB) samples showed better strength than those of CM samples. Surprisingly, strength values were increased without loss of ductility after heat treatment in AM samples. In both as-built and HT conditions, tensile sample built in 45° orientation showed better strength with reasonable ductility when compared to samples built in other orientations. The values of uniform elongation have also shown improvement after heat treatment. The degree of work hardening was also increased after heat treatment in AM and CM samples.

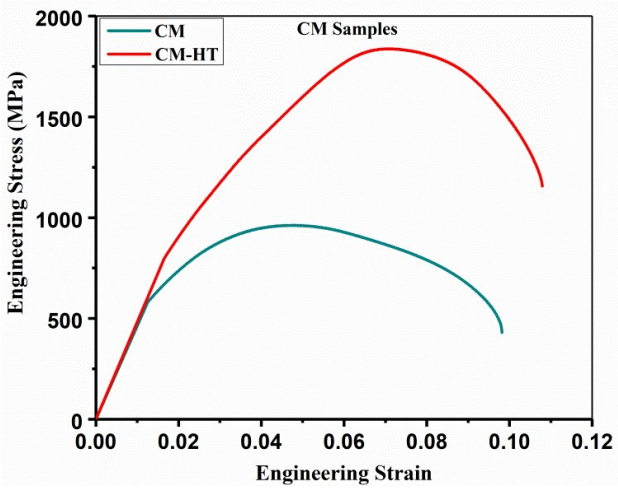

Fig. 4.4 Engineering stress-strain curves of as-received and heat-treated CM samples of M300 steel.

Table.4.2 Tensile properties of AM and CM specimens of M300 steel in different conditions tested at a strain rate of 10^{-3} s^{-1}.

Tensile Samples	Strength Parameters				Ductility Parameters				Degree of Work Hardening	
	AB		HT		AB		HT		AB	HT
	S_y (MPa)	S_u (MPa)	S_y (MPa)	S_u (MPa)	e_f (%)	e_u (%)	e_f (%)	e_u(%)	S_u/S_y	S_u/S_y
0° AM	713	1058	920	1529	11.24	5.08	10.56	5.79	1.48	1.66
45° AM	890	1073	830	1568	10.07	3.84	12.69	7.64	1.21	1.88
90° AM	851	1023	886	1552	9.63	3.26	10.73	7.08	1.20	1.75
CM	581	966	796	1837	10.06	4.98	7.10	3.00	1.66	2.30

S_y=0.2% yield strength, S_u =Ultimate tensile strength, e_f=elongation upto fracture, e_u=uniform elongation.

To analyze the fracture behavior of tensile tested samples, scanning electron microscopy (SEM) of fracture surfaces was undertaken. All the fractographs of as-built (AB) and HT tensile samples are presented in Fig. 4.5. As-built tensile samples in different orientations showed ductile mode of fracture exhibiting dimples due to micro-void coalescence. Some inclusions can also be seen at the bottom of voids as observed in Fig.4.5 (a), (b) and (c). In AB conditions, the voids size and defects were found to be increasing with increase in build orientation. After heat treatment, the mode of fracture remained essentially ductile in all samples. However, the size of dimples was found to be reduced as can be seen in Fig 4.5 (d), (e) and (f). It can also be observed that the size of the voids and number of defects reduced as can be seen from fracture surfaces of HT samples compared to those of AB samples. CM samples also depicted ductile fracture behavior in both heat treatment and as-received conditions.

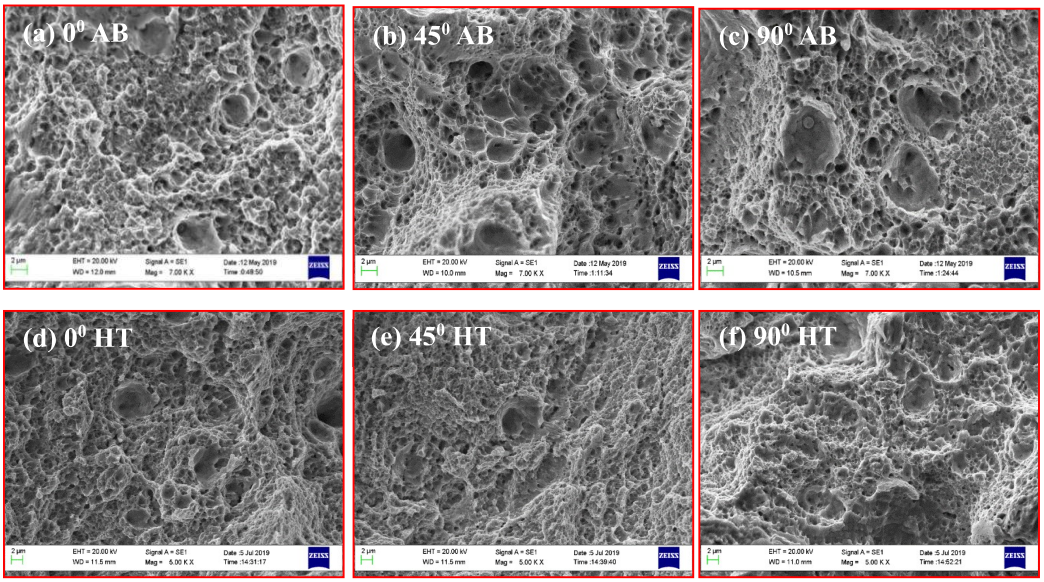

Fig. 4.5 Fractographs of tensile tested specimens in different conditions (a) 0^0 AB (b) 45^0 AB (c) 90^0 AB (d) 0^0 HT (e) 45^0 HT and (f) 90^0 HT.

Strength and ductility anisotropy in tensile results can be analyzed by strength anisotropy (A_{IP}) and ductility anisotropy index (δ). The directionality in tensile properties (Strength and ductility) has been attributed to strength anisotropy and elongation anisotropy index. The results are presented in Table 4.3, where it clearly can be seen that after heat treatment, anisotropy of AM samples due to different build orientations is reduced to a large extent.

Table.4.3 Strength anisotropy (A_{IP}) and elongation anisotropic index (δ) of additive manufactured (AM) as built and heat-treated (HT) samples.

Conditions	Strength Anisotropy A_{IP} (%)	Elongation Anisotropic Index, δ (%)
As built	12	11
Heat treated	8	7

4.3 Influence of Build Orientation on Low Cycle Fatigue Behavior

AM cylindrical rods in different build orientations were machined to required dimensions and mirror polished before testing. The as printed cylindrical rods in different build orientations and the polished LCF samples are shown in Figs. 4.6 (a and b). Uniaxial fatigue testing machine with extensometers and fatigue fractured samples from the gauge section have been shown in Figs. 4.6 (c and d). The schematic diagram depicting orientation of layers and the possible direction of planar defects in different build orientations are shown in Figs. 4.7(a, b and c). The build orientation during SLM affects its cooling rate and consequently its microstructure, whereas the orientation of layers with respect to the loading axis affects the strength parameters as given in Table. 4.2. Existence of voids including pores and un-melted regions between layers (weak metallurgical bonding), due to entrapped gas and low laser penetration depth respectively, have been reported by numerous researchers [135]. Un-melted regions were found to be irregularly shaped and most notably slit-shaped. Consequently, major axes of these defects generally lie along the orientation of layers which can influence the LCF behaviour. Such defects are shown in 0°, 45°, and 90° oriented samples in Figs. 4.7(a), (b), and 4.7(c) respectively.

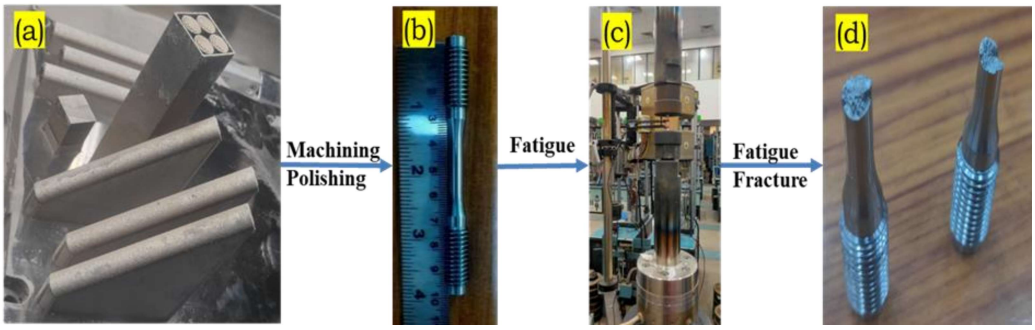

Fig. 4.6. (a) Cylindrical specimens printed via powder bed fusion in 0°, 45°, and 90° build orientation, (b) Machined and polished fatigue samples (c) LCF testing system with extensometer and (d) Fatigue fractured samples.

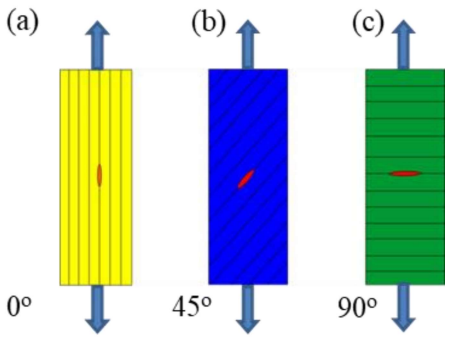

Fig.4.7 Schematic diagram depicting the orientation of layers and the alignment of defects with respect to loading axis in samples built in: (a) 0° (b) 45° and (c) 90° orientations.

4.3.1 Cyclic Stress Response

Fig. 4.8 presents variation of stress amplitude with number of cycles. Fig. 4.8(a) shows comparison of stress response with the number of cycles for AM samples in 0°, 45° and 90° orientations and conventionally manufactured (CM) samples before heat treatment. Similarly, cyclic stress response of heat-treated additive and conventional samples is presented in Fig. 4.8(b).

The stress amplitude may increase or decrease in a very brief initial stage, observable only in the first two or three cycles as shown in Figs. 4.8(a and b). The inconsistent response of stress amplitude, up to two or three cycles, is a result of grip adjustment. Cyclic stress response of samples before heat treatment, in initial stage up to 20 cycles, rapid cyclic hardening can be seen and the stress amplitude reaches maximum. In the second stage, there is a continuous softening up to 90% of the total cycles, further, there is a sudden decrease in stress amplitude with increase in number of cycles and specimen fails at specific number of cycles to failure, N_f. The AB, AM samples exhibited

substantially larger changes in stress amplitude following peak stress amplitude (cycle stabilization, up to 20 cycles) until the number of cycles to failure. This suggests that maraging steel manufactured by AM is more susceptible to cyclic softening prior to heat treatment than conventionally manufactured (CM) samples, presented in Fig. 4.8(a). As built (AB) samples of 45°, showed maximum stress amplitude followed by 90° AB and 0° AB samples in cyclic stress response. The number of cycles to failure (N_f) was found to be decreased with increase in build orientation. AB specimen in 0° orientation exhibited longest fatigue life. Conventionally manufactured (CM) sample in as received condition showed fatigue life (N_f) more than the life observed at 90° AB and less than life at 0° and 45° AB samples. After reaching maximal stress (up to 25 cycles), the HT additive samples exhibited smaller changes in stress amplitude over the entire range of number of cycles [Fig. 4.8(b)]. This indicates that AM specimens are less susceptible to cyclic softening after heat treatment, whereas conventional manufactured heat treated (CM-HT) samples demonstrated cyclic softening.

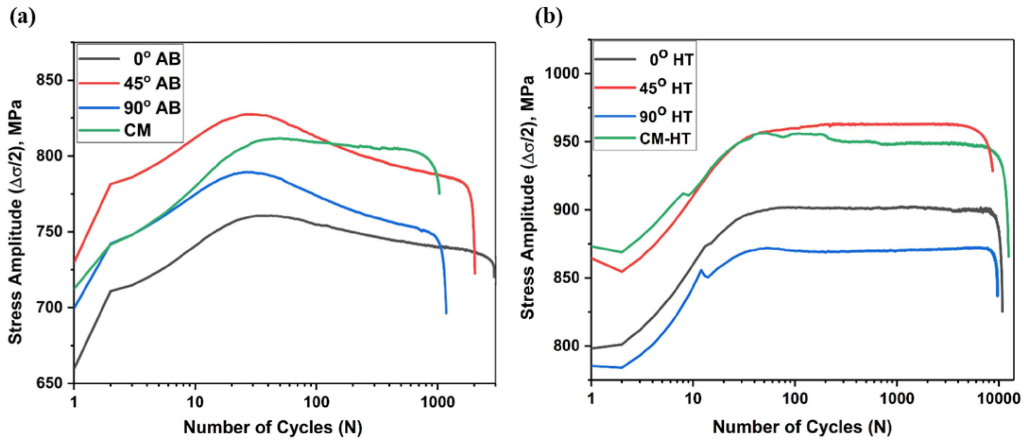

Fig. 4.8 Cyclic stress response of samples at ±0.5% strain amplitude before and after heat treatment: (a) 0°AB, 45°AB, 90°AB and CM samples (b) 0° HT, 45° HT, 90° HT and CM-HT samples.

After heat treatment, strength increased without loss of ductility, due to selected heat treatment. Better strength parameters were observed for 45° HT samples followed by 0°

and 90^o HT samples. 45^o HT samples showed maximum stress amplitude followed by 0^o and 90^o HT samples. There is a sudden increase in stress amplitude up to 20-25 cycles and further stress cycle response gets stabilized. In second stage, there is cyclic softening behavior in 0^0 HT and 90^o HT samples, but in 45^o samples there is a very little continuous cyclic hardening behavior were observed. Similarly, after heat treatment, the number of cycles to failure (N_f) was found to be decreased with increase in build orientation. In Fig 4.8 (b), it can be clearly seen that as built orientation increased the fatigue life decreased. The conventional heat-treated (HT) showed better fatigue life than heat-treated additive samples. After heat treatment the number of cycles for fatigue failure increased when compared to the life of AB additive samples. The fatigue life data of different samples is shown in Table 4.4.

4.3.2 Fatigue life

The number of crack initiation cycles (N_i) was determined using the quotient curve [136]. In this instance, the absolute value of the ratio of compressive to tensile stress (σ_c/σ_t) was plotted against the number of cycles (Fig. 4.9).

Although the majority of this trajectory consists of a plateau, it abruptly rises at the end (Fig. 4.9). In the plateau region, a straight line was fitted, and a parallel line was drawn at a level 3% higher than that of the fitted line. N_i which denotes the number of cycles for crack initiation is determined by the intersection of the parallel line with the quotient curve. The number of cycles for crack propagation (Np) was estimated by subtracting the number of cycles for crack initiation from the total number of cycles to failure (N_f - N_i). From the analysis, it is clear that the LCF life was governed by crack initiation and the results are dependent on build orientation in as-built (AB) and heat treated (HT) AM samples. LCF data for AM and HT samples is given in Table 4.4. It can be seen that as

the build orientation increased, the number of cycles for crack initiation (N_i) decreased both before and after heat treatment. Maximum N_i was observed for conventionally manufactured heat-treated (CM-HT) samples.

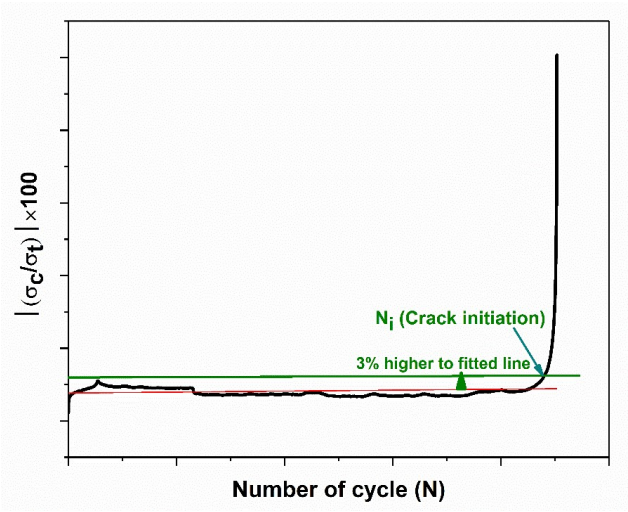

Fig. 4.9. Plots ($|(\sigma_c/\sigma_t)|$ x 100), with the number of cycles and determination of the number of cycles for crack initiation (N_i).

Table 4.4: Fatigue Life of M300 maraging steel in AM and CM conditions.

Build Orientation	As built (AB)/As recieved		Heat Treated (HT)	
	No. of cycle to initiate the cracks (N_i)	Total no. of cycle to failure (N_f)	No. of cycle to initiate the cracks (N_i)	No. of cycle to failure (N_f)
0°	2297	2946	10044	11089
45°	1445	2203	8099	9037
90°	700	1178	7819	8414
CM	1251	1565	11512	12921

4.3.3 Cyclic Hysteresis loops

The area of the hysteresis loops, which represents the plastic strain energy per cycle, can be regarded as a main contributor to the fatigue damage process taking place in each cycle. Fig. 4.10, depicts the (i.e., stable cycle) hysteresis loops at half-life obtained for the as-built and heat-treated additive manufactured samples, as well as the conventional samples. The observed hysteresis loops at $0.5N_f$ in Fig. 4.10(a) reveal that as the build orientation increased from 0° to 90° in AB samples, the percentage of plastic strain energy increased. As-received conventional samples exhibited comparatively less area as compared to the loop area in AB additive samples in 0°, 45° and 90° build orientations. Hysteresis loops at $0.5N_f$ suggest that as the build orientation increased from 0° to 90°, the percentage plastic strain energy increased leading to early fracture. Minimum loop area (% plastic strain energy) was observed for CM samples.

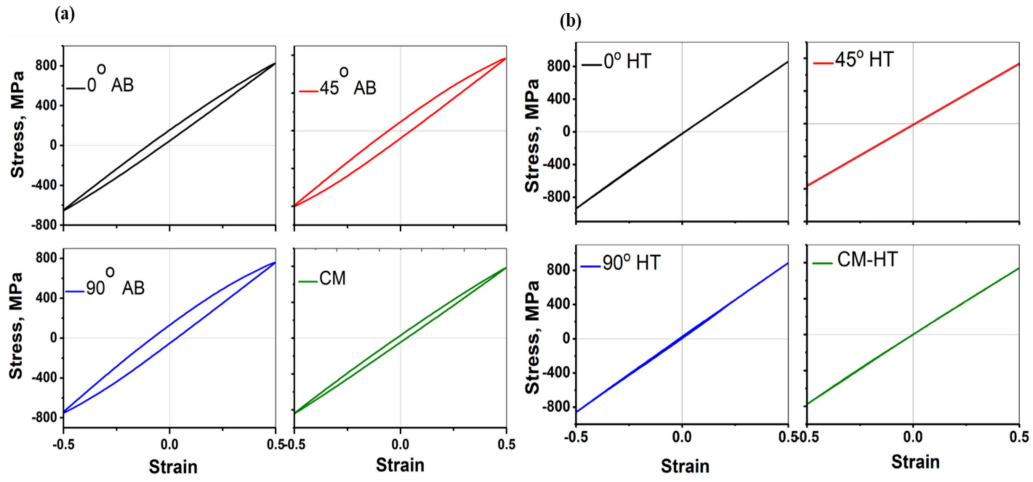

Fig. 4.10 Cyclic stress-strain response of samples before and after heat treatment at $0.5N_f$ cycle and ±0.5% strain amplitude: (a) Hysteresis loops of 0° AB, 45° HT, 90° HT and CM samples and (b) Hysteresis loops of 0° HT, 45° HT, 90° HT and CM-HT samples.

The half-life (i.e., stable cycle) hysteresis loops obtained for the heat treated additive and conventional samples are depicted in Fig. 4.10(b). Hysteresis loop opening of all HT samples are negligible in Fig. 4.10(b), suggest plastic strain at ±0.5% strain amplitude is

very limited. After heat treatment strength parameter increased significantly and ±0.5% strain amplitude impart stress just above the yield strength. From Fig. 4.10(b), it is clear that 90° HT sample showed comparatively more plastic strain energy than other heat-treated samples.

4.3.4 Fracture behaviour of LCF tested samples

Fig. 4.11 presents fractographs of the 0° AB and 45° AB samples failed by fatigue. Multiple crack initiation sites can be seen at lower magnifications as shown in Figs. 4.11(a and d). Further at higher magnifications, gas pores/voids can be seen in 0° AB samples [(Figs. 4.11(b and c)], which can act as internal crack initiation sites. Striations around pores are clearly visible. In 45° AB samples, at higher magnifications, striations along with pores can be observed [Figs. 4.11(e and f)]

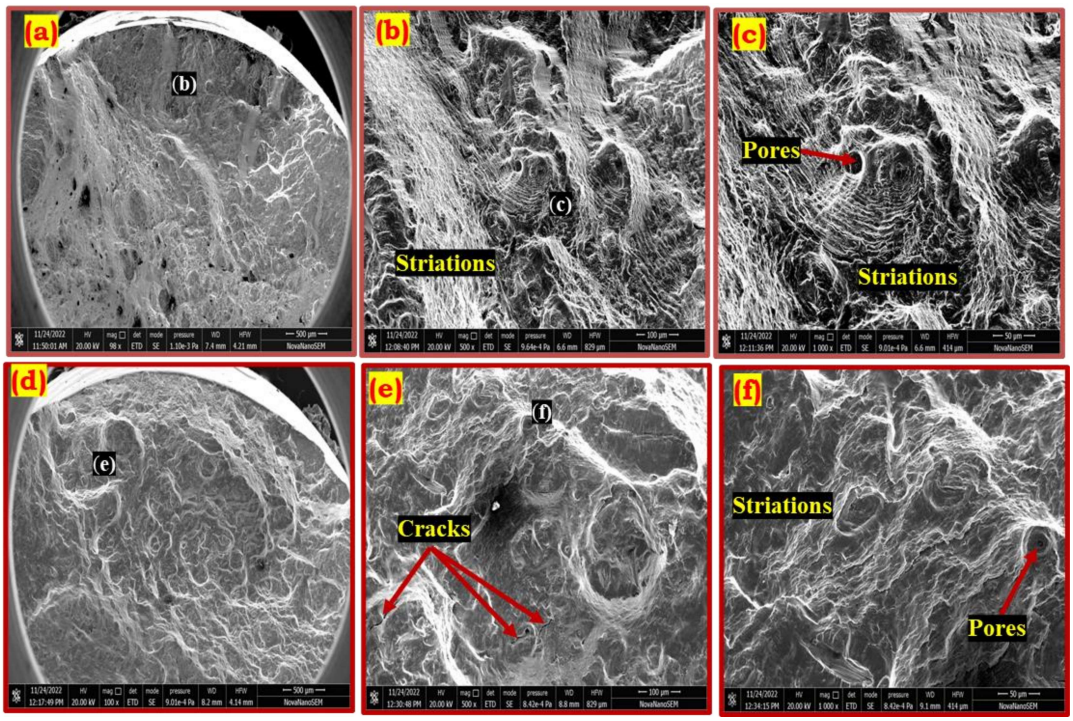

Fig. 4.11 Fractographs of fatigue tested samples: (a-c) 0° AB and (d-f) 45° AB.

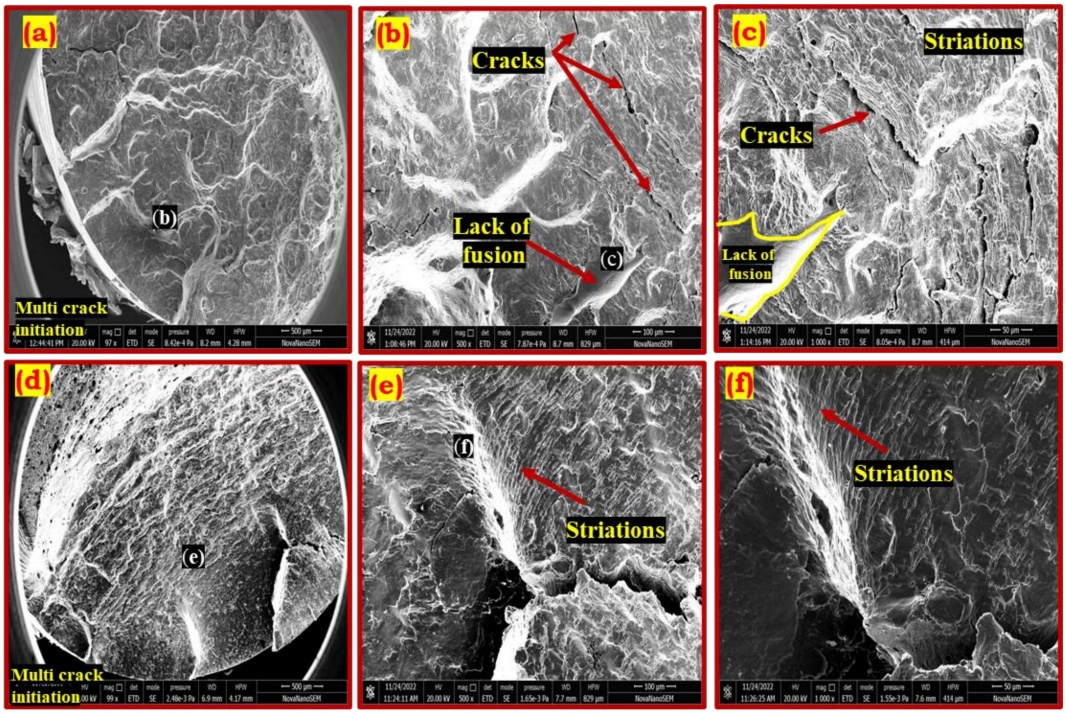

Fig.4.12 Fractographs of fatigue tested samples: (a-c) 90° AB and (d-f) CM sample.

At lower magnifications, in Figs. 4.12 (a and d), multiple crack initiation sites, in 90° AB and conventional as received (CM) sample were observed. Further at, higher magnifications, lack of fusion defects with pores can be noticed. In Figs. 4.12(c and f), the characteristic fatigue features i.e., clear striations can be seen, while in 90° AB samples, internal cracks can be observed. The conventional manufactured (CM) sample showed very clear striations characteristic of fatigue failure with no internal defects as shown in Figs. 4.12(e and f).

The fractographs of HT samples of 0° and 45° are shown in Fig. 4.13, in which it can be clearly observed that 0° HT samples depicted single crack initiation site as in Fig 4.13(a), while 45° HT samples exhibited multiple crack initiation sites as in Fig. 4.13(d). Further at higher magnifications, no clear voids and lack of fusion were found and very fine striations can be observed in both 0° HT and 45° HT samples. The 45° HT samples also

exhibited clear lack of fusion defects near the surface from where the fracture was initiated, as marked in Fig. 4.13(f).

The fractographs of HT samples of 90° and CM-HT are given in Fig. 4.14. It can be clearly observed that 90° HT samples revealed multi crack initiation sites as in Fig 4.14(a), while CM-HT samples depicted single crack initiation site as shown in Fig.4.14(d). Further at higher magnifications, no clear voids and lack of fusion were observed in both 90° HT and CM-HT samples. A clear fatigue signature (i.e., striations) was observed in HT conventional sample, as presented in Fig. 4.14(f). Clear striations marks were not observed in HT additive samples.

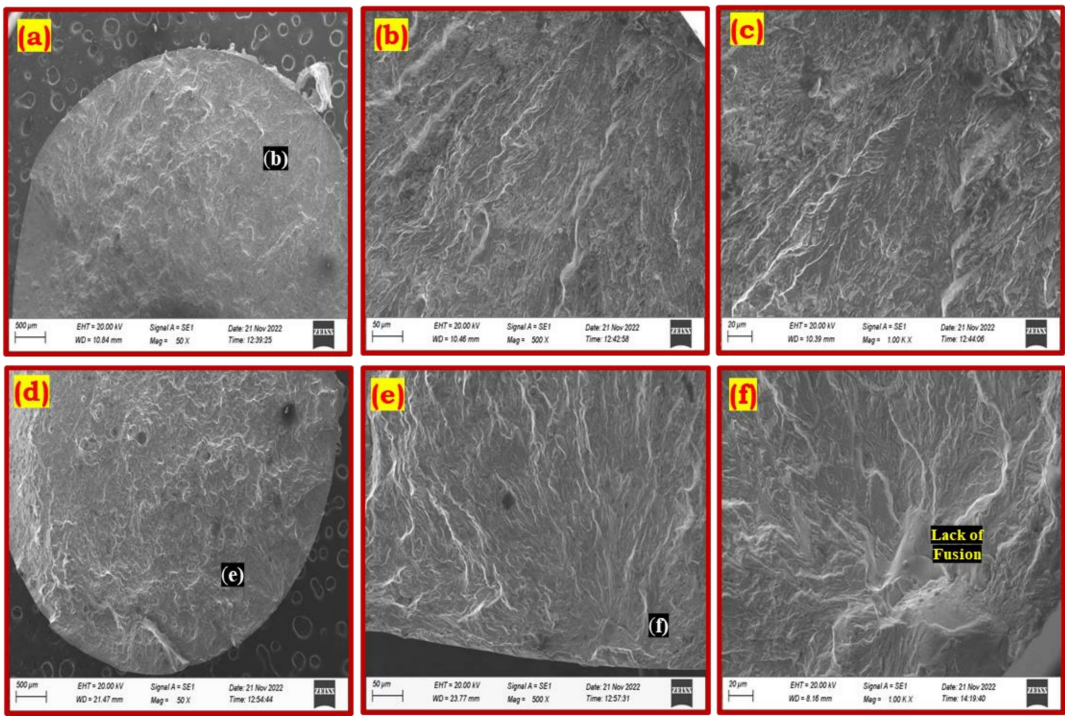

Fig. 4.13 Fractographs of fatigue tested samples: (a-c) 0° HT and (d-f) 45° HT.

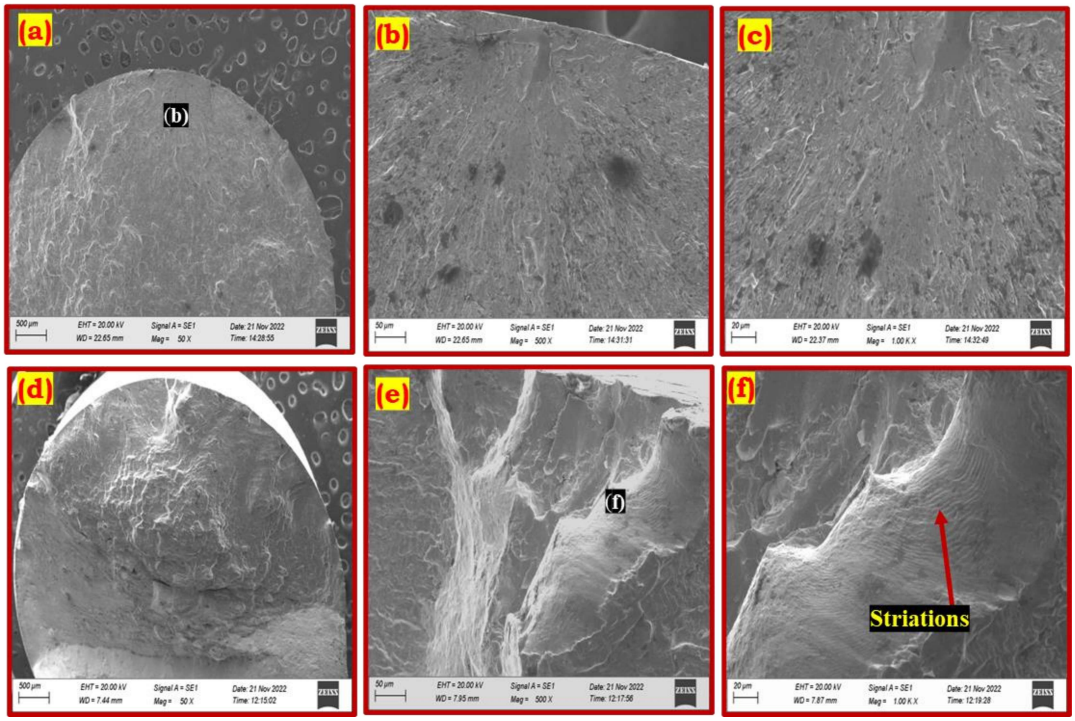

Fig. 4.14 Fractographs of fatigue tested samples: (a-c) 90^{o} HT and (d-f) CM-HT.

4.4 DISCUSSION

4.4.1 Residual stresses

Residual stresses were generated during the start of solidification of molten layer in AM, mainly due to solidification-induced shrinkage and thermal gradients [137]. Powder surrounding the processed specimens and base plate act as heat sinks. It is found that contact area (heat transfer surfaces) with the base plate is maximum in 0◦ orientation followed by 45◦ and 90◦ processed specimens. As a consequent result, the heat transfer rate is found to be maximum in 0◦ followed by 45◦ and 90◦ oriented samples. Also, longer time for a given layer helps the specimen to dissipate heat rapidly and cool faster after processing. In the present case, specimens built in 0◦ orientation had the longest layer time followed by those produced in 45◦ and 90◦ orientations [138, 139]. It is also observed that residual stresses often transfer into the base plate either by direct contact

or through support structure. Parts built with maximum contact with the base plate (direct or support structure) are found to warp less and have lower residual stresses. Plate built in 90^{o} orientation usually has minimum contact with the base plate. Another important factor is the residual heat in the layers of the part produced. More the residual heat remained in the part, more are the residual stresses. Also, longer time for a given layer helps the part to cool more after processing and can impart residual stresses. In the present case, plate built in 0^{o} orientation has longest layer time followed by those produced in 45^{o} and 90^{o} orientations. As the layer time for sample in 90^{o} orientation was less, excessive heat was built up thus leading to the generation of maximum residual stresses. Tan et al. [61] showed that in SLM processed materials, residual stress reaches its highest value on top surface. Formation of the residual stress can be understood with two mechanisms namely, cool down mechanism and thermal gradient mechanism (TGM). TGM deals with the residual stresses generated in single track while cool down mechanism takes into account residual stresses generated in bulk [140]. During processing of powders, large thermal gradients around the laser spot are formed due to intense heating in a very fine local region that results in TGM which causes bending of sheet along laser track. Processing of powder layer by layer in SLM, top layer gets heated due to which it expands but under lying layers act as a constraint for top heated layer with the results it imposes compressive strain on top layer. 67^{o} inter layer rotation can also contribute to the generation of compressive residual stresses, because bending and shrinkage while cooling could suppress and counteracted with the rotation of laser heat flux [141]. The residual stresses found in the present work are compressive in nature and got relieved after heat treatment due to thermal recovery.

4.4.2 Hardness

Because of higher rate of heat transfer, the as-built AM samples have fine cellular structure whereas the as-received conventional (CM) sample shows coarse and equiaxed microstructure. As a consequence, as-built AM samples showed better hardness values than those of CM samples [142]. The 90° AB sample showed maximum hardness, because it had maximum residual stress among all other samples in different orientations. Solution treatment (ST) of AB samples relieves the cellular structure, segregation and residual stresses which cause easy mobility of dislocations that results in lower hardness than the values exhibited by CM as fabricated samples [143]. After HT, the hardness of CM and AM samples increased due to the contribution of age hardening. In HT samples, improvement in hardness could be also due to the precipitation of the Ni_3Ti and Fe_2Mo. However, the formation of the reverted austenite because of over aging might have caused some reduction in hardness [64].

4.4.3 Tensile behaviour

Figures 4.2 and 4.3 depict the tensile properties of 0°, 45° and 90° oriented AM specimens in their as-built (AB) or heat treated (HT) states. According to the results, the monotonic tensile behaviour of AM maraging steel is significantly affected by building orientation and post-heat treatment (solution annealing plus ageing). The yield and ultimate tensile strengths were substantially affected by the post-heat treatment, whereas the elongation to failure was primarily influenced by the orientation of the part in AB conditions and phase fraction (reverted austenite) in HT conditions. The effects of heat treatment on the investigated AM components are attributed to the formation of precipitates in the martensite matrix, as well as the modification of other microstructural features, i.e., phase volume fraction, grain size, and morphology, whereas the build orientation has a direct influence on the damage evolution under loading. Due to inherent layer-wise processing

method of AM, the specimens built in different orientations (0^o, 45^o and 90^o) exhibited slight anisotropy in tensile properties. After HT, the anisotropy gets reduced because of formation of isotropic microstructure, onset of precipitation and relieve of residual stresses. The 45^o HT sample showed highest ductility due to the larger volume fraction of reverted austenite. As received CM samples showed lowest strength among all the tensile samples tested due to coarse and equiaxed grains. It is surprising that after heat treatment, the CM tensile sample showed highest ultimate tensile strength among all the samples. Precipitation along with large degree of work hardening might have contributed to the reported value of UTS. Large dimples were observed in as-built (AB) tensile samples with comparatively larger micro voids than those in HT tensile samples of different orientations with less homogeneity in structure and lower ductility, consistent with the earlier reports [144]. The tensile study reveals that the samples built in the 45° orientations exhibit better strength and reasonable ductility compared to those at other build orientations (0^o and 90^o), and the material in CM conditions. The microstructural anisotropy caused by layer-wise effect due to laser processing is reduced by the solution treatment followed by aging. Moreover, most of the AM samples after heat treatment show an increase in strength without significant loss in ductility. This behavior can be attributed to a larger degree of work hardening and reversion of martensite to austenite. After heat treatment, precipitation and austenite reversion take place which affect the tensile properties. Austenite is easily deformable as compared to martensite. The percentage of reverted austenite is different in different orientations, which might have contributed to different values of YS in HT samples as can be seen in Table 4.2. However, UTS values which represent maximum strength values that a specimen can exhibit, are not affected, as these values (reverted austenite) are very close to one another. Austenite is easily deformable as compared to martensite. Therefore, significant change in uniform

elongation was observed after heat treatment due to reverted austenite. Ductile fracture featuring dimples due to microvoid coalescence is observed in all the samples. The heat treatment not only improves the mechanical properties but also reduces anisotropy and residual stresses introduced during material processing.

4.4.4 Low Cycle Fatigue Behaviour

For a 90^o oriented specimen, the major axis of a split-shaped un-melted region (defects due to AM processing) is perpendicular to the loading axis; however, in 0^o and 45^o oriented specimens, the major axis of an un-melted region is orientated parallel and at 45^o to loading axis respectively, as demonstrated schematically in Fig. 4.7. Thus, the stress concentration of an un-melted region, in which the major axis orientated perpendicular to the load direction (such as 90^o oriented samples), is several times higher, and consequently, more prone to opening and initiating cracks. As a result, under uniaxial fatigue testing, horizontal specimens (0^o) showed longer fatigue lives as indicated in Fig. 4.8(a) and Table 4.4, followed by 45^o and 90^o oriented samples. In LCF tested samples in AM conditions, initially there is cyclic hardening followed by cyclic softening and fracture. There is a rapid drop in cyclic stress amplitude i.e cyclic softening primarily due to initiations of cracks at multiple locations and their propagation to final fracture. In the absence of voids and inclusions, slip bands usually drive crack initiation in conventionally manufactured (CM) samples [145]. In general, finer microstructures formed in as-built AM samples due to high solidifications rates, provide better crack initiation resistance than coarser microstructures i.e., in conventional as received samples and for this reason, before heat treatment, the conventional samples showed lower fatigue life than the lives exhibited by additive samples. After heat treatment, intermetallic precipitates, mainly Ni_3Ti, Fe_2Mo and reverted austenite were observed in the matrix which increase the strength parameters (i.e., tensile strength without loss of ductility),

and consequently, cause more resistance to dislocation movement, which results in its enhanced resistance to crack initiation and improved fatigue life in heat-treated samples as shown in Fig. 4.8(b) and Table 4.4 [146]. In the current study, the samples were first solutionized at 815^{o} C for 1 hr, forming a lath martensitic matrix. Further aging at 520^{o} C for 5 hr resulted in the formation of precipitates in the martensite matrix. Due to slight over aging temperature given in the present work, the intermetallic precipitates got coarsened which might have resulted in the reduction of size and quantity of defects. Build orientation anisotropy in fatigue life was maintained even after heat treatment. This is due to structural anisotropy in AM parts may be more influenced by defects rather than microstructure [147]. The area of the hysteresis loops, which represents the plastic strain energy per cycle, can be regarded as a main contributor to the fatigue damage process taking place in each cycle and as expected 90^{o} AB samples showed more plastic strain followed by 45^{o} AB and 0^{o} AB samples, as presented in Fig. 4.10(a). HT specimens did not show significant plastic deformation even at ±0.5% strain amplitude since strength parameters improved drastically after heat treatment, thus hysteresis loops of HT samples show a single line as given in Fig. 4.10(b). Cracks are generally initiated at microstructural defects (i.e. voids and particles) and grain boundaries. Due to the presence of a large number of impurities with various size, shape, and location, they serve as crack initiation sites in AM specimens. Therefore, multiple cracks got initiated which can readily progress and coalesce into final fracture. In 90^{o} AB samples, fractograph depicts large and irregular shape lack of fusion defects which can readily open because the defect axis is perpendicular to loading axis. Hence crack propagation life was lowered in 90^{o} AB samples than those of horizontal samples. After heat treatment, formation of large number of precipitates and reduction in size and number of defects were observed. This helped in major enhancement in fatigue life of heat-treated samples. Un-melted

regions resulting from processing by PBF-LB, such as lack of fusions and voids, are found to be the most detrimental type of defects on fatigue life due to their relatively large size and irregular shape [148]. These specific defects that formed during fabrication of 90° orientated samples are more detrimental than those of 45° and 0° orientated ones as they provide more stress concentration under loading, leading to lower fatigue life. Finally, the SEM analysis shows that for almost all the tested samples, cracks initiate from the surface and inner defects which propagate through the rest of the cross-section and lead to final failure.

4.5 CHAPTER SUMMARY

A detailed study was carried out on tensile and low cycle fatigue behaviour of additively manufactured maraging steel in as-built and heat-treated conditions and compared with conventional manufactured maraging steel. The effect of build orientations anisotropy is also investigated in tensile and fatigue results. Important conclusions are mentioned below.

1. The compressive residual stresses varied with built orientations which increase with increase in orientation. After heat treatment, most of the stresses were relieved due to thermal recovery.
2. In addition to residual stresses in as-built condition, precipitation and austenite reversion due to heat treatment also significantly affected the hardness and tensile properties of M300 maraging steel. Large volume fraction of reverted austenite led to significant ductility in 45° oriented heat-treated samples.
3. Large degree of work hardening along with precipitation contributed to the highest value of ultimate tensile strength of CM samples after heat treatment.
4. Fractography of tensile tested samples depicted mainly ductile fracture in the as-built and heat-treated samples.

5. Fatigue properties of samples are governed by orientation of defects to loading axis. 90^{o} oriented samples showed minimum fatigue life in both as built (AB) and heat-treated (HT) conditions.
6. There is a cyclic softening behaviour in AB samples and after heat treatment, more stable cyclic response was observed in all conditions with small degree of cyclic hardening.
7. The fracture surfaces revealed multiple crack initiation sites in both AB and HT samples. In 90^{o} AB samples, large and irregular shaped defects due to lack of fusion were observed.
8. The fatigue life of additive samples was found to be mainly governed by processing defects (voids and lack of fusion) rather than microstructure.
9. Post heat treatment (HT) was found to be very effective to improve fatigue life and major enhancement in fatigue life was observed due to formation of precipitates and reduction in size and number of defects.